IEEE *Access*

Fault Current Negative Contribution Method for Inverter-Based Distributed Generators Under Grid Unbalanced Fault

XUBIN LIU[ID]

School of Electrical and Electronic Engineering, Huazhong University of Science and Technology, Wuhan 430074, China

e-mail: liuxubin@hust.edu.cn

ABSTRACT With the rapid increase of embedded inverter-based distributed generators (IBDGs), the active distributed network (ADN) is facing security and protection challenges because IBDGs will contribute extra fault current. In contrary to the existing method that IBDGs provide varying degrees of positive contribution to system fault current, in this article, a fault current negative contribution (FCNC) method is proposed for IBDGs to reduce the system fault current lower than the situation where without IBDGs embedded. In the proposed method, a maximum current phase angle adjustment (MCPAA) strategy is conducted for IBDGs to maximize its negative contribution, thus to minimize the system fault current. In order to obtain a more precise current phase angle, a voltage phase angle determination (VPAD) strategy is also formulated by considering the voltage angle difference on the electrical distance between IBDGs and fault bus. Extensive tests and relevant results have validated the feasibility of FCNC method to achieve a negative contribution of IBDGs on system fault current.

INDEX TERMS Fault current limit, active distributed generator, inverter, phase angel adjustment, unbalanced fault.

I. INTRODUCTION

Driven by the energy shortage, environmental pollution, and economic issues, the renewable energies, such as solar and wind power, combined with the electrochemical energy storage systems, such as batteries, are widely integrated into the active distribution network (ADN) in the form of IBDGs [1], [2]. With the increasing penetration of IBDGs, its advantages to the DN are universally acknowledged, such as reliability, economy and flexibility [2]. However, at the same time, some serious safety and protection concerns caused by IBDGs has also raised, especially under the DN fault condition [3]–[5]. One of the most serious bottlenecks is related to the high-level fault current, since the utility grid and all IBDGs will contribute the fault current into the fault bus together [3]–[5].

It is important to reduce the high-level system fault current under grid fault condition, otherwise, the fault current will cause some serious consequences to AND [6]–[14]: 1) The ever-increasing fault current makes the power equipment faces higher dynamic and thermal stability requirements [6].

The larger the fault current, the higher the capacity of the grid equipment is needed to improve electrical stability [7]; 2) The increasing fault current will speed up the replacement of grid equipment, thus increase the grid investment, since the electrical equipment is planned and designed based on its ability to withstand fault currents [8]; 3) The IBDGs fault current will interfere the coordination operation between the primary protection and secondary protection of the original relay protection of ADN, increasing the difficulty of coordination between protection and reclosing [9]–[10]; 4) The IBDGs fault current will lead to a certain sensitivity reduction of the related overcurrent protective relay, and even cause protection blinding or false tripping of related relay [11]–[13]; 5) With the increase in the capacity and scale of IBDGs, the ADN is facing the danger of excessive fault current [14]. Once the fault current cannot be removed by circuit breakers, the fault current can even cause cascading fault [15]. In summary, the ever-increasing level of fault current in the ADN has become one of the main bottlenecks restricting the security and stable of power system.

It is a challenge to manage and limit the sharp increase of fault current in ADN. Considering that the ADN can not shake and adjust the fault current injected from utility grid's

conventional synchronous generator, while the IBDGs fault current in AND is an additional emerging and unfavorable current when compared with the traditional passive DN, the most direct and effective method is to adjust the IBDGs fault current [3]–[5], [7], [16].

Numerous studies have been studied to manage the impact of IBDGs fault current under grid fault condition. Traditionally, according to IEEE Std 1547−2003 [17], IEEE Std 929−2000 [18] and UL 1741−1999 [19], the IBDGs are forcibly disconnected from grid when fault occurs in ADN. Thus, the IBDGs fault current does not exist anymore. However, with the increase capacity and scale, the IBDGs are required to maintain connected with grid during fault condition [1], [2]. Thus, the low-voltage ride-through (LVRT) or fault ride-through (FRT) is established, such as German E.ON NetZ code, UK National grid code, USA and China grid code [20]–[22]. Then, the voltage support of IBDGs is also developed, such as international standards [23]. In order to reduce the IBDGs fault current during LVRT/FRT and voltage support, there are two main methods here. One is to install additional fault current limiting equipment. For example, the fault current limiters (FCLs) [24], [25]. The FCLs are developed with a common feature of near-zero impedance in normal operations and a high impedance in fault operations to block the flow of fault current. The typical FCLs includes solid-state, magnetic, and liquid-metal [26], [27]. The other is to design the suitable fault current limiting strategies for the inverters of IBDGs. In particular, the peak current limiting strategy under balanced and unbalanced fault is proposed for IBDGs [28]–[30]. The starting point of these methods is mainly to limit the inverter output current lower than 2∼3 times the rated current of the unit, due to the semiconductor safety constraints [3], [4]. However, these methods will increase the system fault current [24]–[30]. To eliminate the IBDGs' influence on the system total fault current, the adjustment for the phase angle of IBDGs fault current is also proposed recently [3]–[5], [7], [16]. Then, the positive contribution of IBDGs on system fault current can be reduced.

However, all the above existing methods will make IBDGs provide varying degrees of positive contribution to system fault current. It is imperative to find a method to make IBDGs provide negative contribution of fault current on system. Thus, it will be benefit for utility grid due to the reduced harmful of fault current. According to the flexible control characteristics of IBDGs inverter for the output voltage and current, the suitable output current phase angle adjustment will be completely feasible [3]–[5], [7], [16]. Based on the current phase angle superposition characteristics, appropriate current phase angle can transfer IBDGs fault current from positive contribution to negative contribution.

In this article, the motivation is how to reduce the system fault current of ADNs by the control of IBDGs, making the total fault current lower than it's in situation when without IBDGs embedded. To solve this challenge, a fault current negative contribution (FCNC) method is proposed
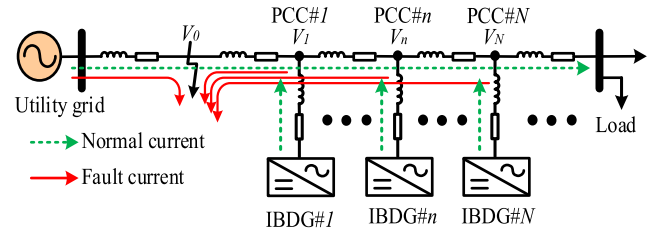

FIGURE 1. The structure of IBDGs embedded in ADN and the related normal and fault current flow.

for IBDGs. The major contributions are summarized as:

1) A maximum current phase angle adjustment (MCPAA) strategy is conducted for IBDGs to maximize its negative contribution, thus to minimize the system fault current;

2) A voltage phase angle determination (VPAD) strategy is formulated by considering the voltage angle difference on the electrical distance between IBDGs and fault bus, thus to obtain a more accurate value of current phase angle.

The remainder of this article is arranged as follows. The fault current injecting characteristic of IBDGs and utility grid is modeled in Section II. An FCNC method consists of MCPAA, VPAD and ICG strategies is formulated in Section III. Numerous case studies for system fault current limiting are developed in Section IV. The conclusions are provided in Section V.

II. FAULT CURRENT CHARACTERISTIC ANALYSES DURING GRID FAULT

During grid fault, both utility grid and IBDGs will inject the fault current. In order to achieve a negative contribution of IBDGs fault current, there has to be advance analysis the phase angle injecting characteristic of both utility grid and IBDGs fault current under grid fault.

A. FAULT CURRENT INJECTING ANALYSES

The topology structure of ADN embedded with IBDGs and the related normal and fault currents injecting are displayed in Fig. 1. In normal condition, the current needed for load is provided by utility grid and all IBDGs. In fault condition, since the IBDGs is maintained in grid-connected state, the fault current in fault point is also injected from utility grid and all IBDGs. Due to the current exported by the embedded of IBDGs, the system fault current in ADN with IBDGs will be much high than that in case without IBDGs in traditional DN. Considering the adjustable ability of IBDGs output voltage and current, the limitation of system total fault current mainly depends on the control of IBDGs output fault current.

The IBDGs fault current will be influenced by the fault bus voltage (V_0), PCC voltage (V_n), and the electrical distance line impedance. The control of IBDGs fault current should take into account these factors on the base of phase angle superposition characteristic.
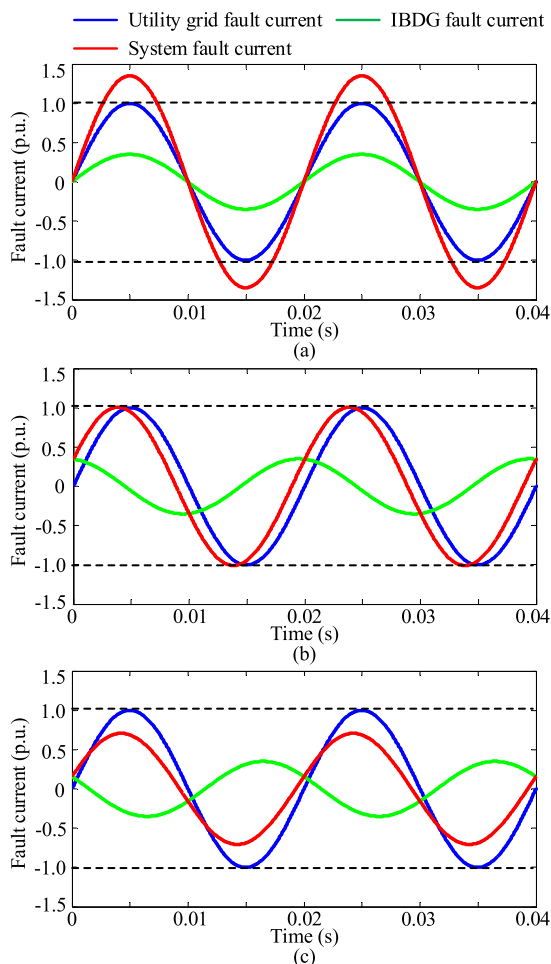
FIGURE 2. The system fault current: (a) IBDGs fault current with positive contribution and without phase angle adjustment; (b) IBDGs fault current with no contribution by phase angle adjustment; (c) IBDGs fault current with negative contribution by phase angle adjustment.

B. FAULT CURRENT PHASE ANGLE ANALYSES

Based on the analyses of Fig. 1, the utility grid fault current is uncontrollable, while the IBDGs fault current is controllable. Thus, the system fault current limiting mainly relies on the control of IBDGs fault current.

The IBDGs fault current has both amplitude and phase angle controllable variables. According to the phase superposition characteristics, the system fault current can be limited to different degrees (larger, equal and smaller than utility grid fault current) by controlling the phase angle value of IBDGs output current. The amplitude features of fault current based on different phased angle control of IBDGs output current is shown in Fig. 2. Based on Fig. 2(a), if the IBDG output current is not controlled, the system fault current is much high than the injected utility grid fault current, and the IBDG output current has a positive contribution on the system fault current. Based on Fig. 2(b), if the angle of IBDG output current is controlled to a certain value, the amplitude of system fault current is equal to that in utility grid fault current, and the IBDG output current has no influence on the system fault current. Based on Fig. 2(c), if the angle of

IBDG output current is controlled to a certain larger value, the amplitude of system fault current is lower than that in utility grid fault current, and the IBDG output current has a negative contribution on the system fault current.

Based on the above analyses, the Fig. 2(a) will be a bad scenario, since the system fault current in ADN is larger than it's in traditional DN without embedded IBDGs. Thus, it is easy to cause protection failure and cause safety problems. The Fig. 2(b) is the most neutral scenario, since the system fault current in ADN is equal to it's in traditional DN. The IBDGs will not affect the relay protection based on the overcurrent amplitude protection. The Fig. 2(c) will become ideal scenario, since the system fault current in ADN is lower than it's in traditional DN. It means that the IBDGs can help the relay protection of power system. Therefore, it will be significant to find the suitable phase angel in Fig. 2(c).

III. FAULT CURRENT NEGATIVE CONTRIBUTION METHOD FOR IBDGs DURING GRID FAULT

Based on the analyses in Section II, a fault current negative contribution (FCNC) method is proposed to find the maximum phase angle in Fig. 2(c), in order to minimize the system fault current. To quantify this precise phase angle, the FCNC method contains maximum current phase angle adjustment (MCPAA) strategy and voltage phase angle determination (VPAD) strategy. In order to match the function of MCPAA and VPAD, the inverter current generation (ICG) strategy is also developed.

A. MCPAA STRATEGY

Taking one IBDG as an example, the IBDG output fault current vector under the scenario of positive, negative and no contribution is show in Fig. 3. Take positive sequence as an example, the system fault current (I_F) is injected by utility grid fault current (I_{UG}) and IBDG fault current (I_{IBDG}).

According to Fig. 3(a), when the phase angle of IBDG output fault current is different, the IBDG output fault current has positive, negative and no contribution on system fault current, corresponding to the phase angel region of IBDG fault current in *OAB*, *OBC* and *OB*, respectively. Specifically, if the angle of IBDG output fault current is not adjusted additionally, the amplitude of system fault current is highest, and the fault clearing is most difficult. This scenario corresponds to point *A*. If the angle region of IBDG fault current is distributed in *OAB*, the IBDG has positive contribution on system fault current, since the system fault current amplitude is higher than utility grid fault current. If the angel is shifted to point *B*, the system fault current amplitude is the same as the utility grid fault current, thus the IBDG has no contribution on system fault current. If the angle region of IBDG fault current is distributed in *OBC*, the system fault current amplitude is lower than utility grid fault current, thus the IBDG has negative contribution.

Based on Fig. 3(b), the system fault current is the subtraction of utility grid fault current and IBDG fault current. The ideal situation lies that the angle of IBDG fault current is opposite to the utility grid fault current. Thus, the system
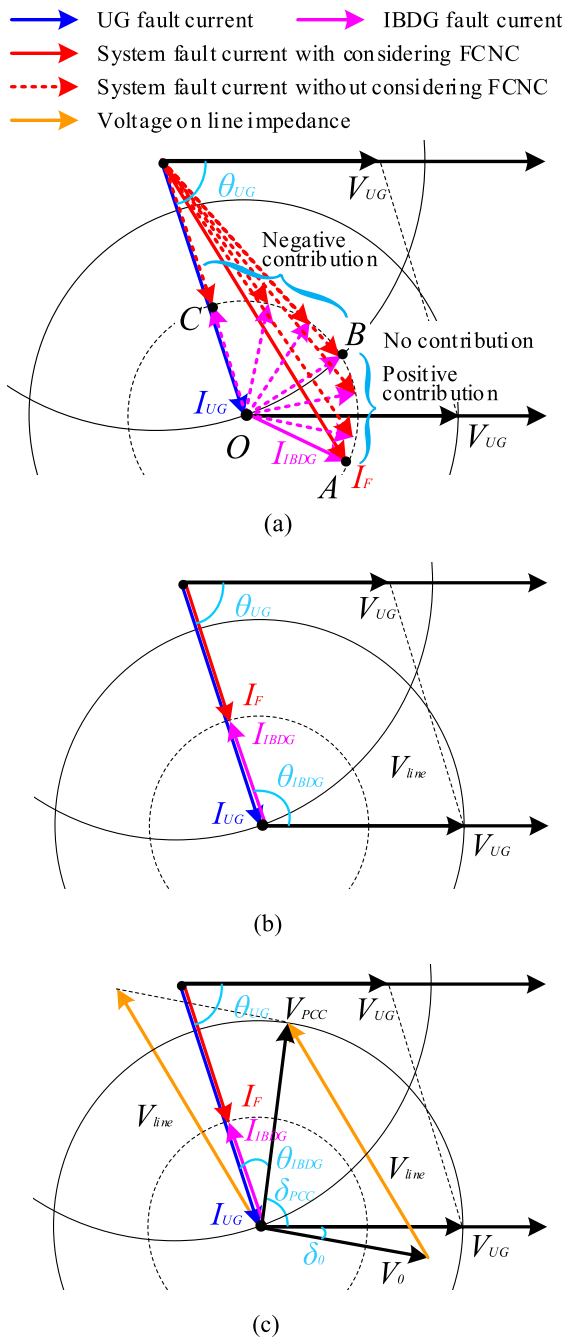
FIGURE 3. Fault voltage and current vector analyses: (a) IBDGs fault current with positive, negative and no contribution to the system fault current; (b) vector analyses for MCPAA strategy; (c) vector analyses for VPAD strategy.

fault current is smallest. In this situation, the phase angel of IBDG fault current is optimal, and the IBDG has a maximum negative contribution on system fault current. The situation when the angle of IBDG output fault current is opposite to utility fault current, is call by MCPAA strategy in proposed FCNC method.

Based on Fig. 3(b), the vector relationship of system fault current with MCPAA strategy is described as

$$\vec{I}_{UG}^{+/-} + \vec{I}_{IBDG}^{+/-} = \vec{I}_F^{+/-} \tag{1}$$

where $\vec{I}_{UG}^{+/-}$, $\vec{I}_{IBDG}^{+/-}$ and $\vec{I}_F^{+/-}$ are the vector of positive and negative sequence of utility grid fault current, IBDG fault current and system fault current, respectively.

The amplitude has the following relationship as

$$\hat{I}_F^{+/-} = \hat{I}_{UG}^{+/-} - \hat{I}_{IBDG}^{+/-} \tag{2}$$

where $\hat{I}_{UG}^{+/-}$, $\hat{I}_{IBDG}^{+/-}$ and $\hat{I}_F^{+/-}$ are the amplitude of positive and negative sequence of utility grid fault current, IBDG fault current and system fault current, respectively.

According to (2), the (1) is rewritten as

$$\begin{cases} \hat{I}_{UG}^{+/-} \cos(\theta_{UG}^{+/-}) + \hat{I}_{IBDG}^{+/-} \cos(\theta_{IBDG}^{+/-}) \\ \quad = (\hat{I}_{UG}^{+/-} - \hat{I}_{IBDG}^{+/-}) \cos(\theta_{UG}^{+/-}) \\ \hat{I}_{UG}^{+/-} \sin(\theta_{UG}^{+/-}) + \hat{I}_{IBDG}^{+/-} \sin(\theta_{IBDG}^{+/-}) \\ \quad = (\hat{I}_{UG}^{+/-} - \hat{I}_{IBDG}^{+/-}) \sin(\theta_{UG}^{+/-}) \end{cases} \tag{3}$$

where $\theta_{UG}^{+/-}$ and $\theta_{IBDG}^{+/-}$ are the phase angle of positive and negative sequence of utility grid fault current, IBDG fault current, respectively.

Based on the mathematical relationship in (3) and the graphics relationship in Fig. 3(b), the angle of IBDG and utility grid fault current can be expressed as

$$\theta_{UG}^{+/-} + \theta_{IBDG}^{+/-} = 180° \tag{4}$$

Then, the MCPAA of IBDG fault current is expressed as

$$\theta_{IBDG}^{+/-} = 180° - \theta_{UG}^{+/-} \tag{5}$$

B. VPAD STRATEGY

According to the analysis in Section III.A, Fig. 3(b) and (5), it is obvious that the phase angle calculation for MCPAA is inaccurate, since the phase angle of fault voltage and PCC voltage is ignored. According to the Fig. 1, the fault voltage will be affected by electrical distance line impedance. In addition, according to the Fig. 3(c), when considering the electrical distance, the fault voltage (V_0) and PCC voltage (V_{PCC}) is different. The amplitude of fault voltage at fault bus (V_0) is less than normal grid voltage (V_{UG}). However, the IBDGs should be required to be connected with grid under fault condition, and play the role of auxiliary service for voltage compensation. Thus, amplitude of PCC voltage (V_{PCC}) is equal to normal grid voltage (V_{UG}), but the phase angle of PCC voltage V_{PCC} will be ahead of V_{UG}.

Compare with the angle of utility grid voltage (V_{UG}), the angle of fault voltage (V_0) will lag δ_0 than V_{UG}. The PCC voltage (V_{PCC}) will be ahead of δ_{PCC} than V_{UG}. The voltage on the electrical distance line impedance is V_{line}, which is used to support the V_0 to V_{PCC}. The phase angel of V_{line} is ahead of I_{IBDG}, since the line impedance is resistance and inductance type.

Different from conventional positive contribution, for the purpose to achieve a negative contribution of IBDG fault current, the key is to make phase angel of V_{PCC} (δ_{PCC}) be ahead of both fault bus's fault voltage V_0 (δ_0) and utility grid voltage V_{UG}.

According to the above analysis and the graphics relationship in Fig. 3(b)-(c), and (5), the revised phase angle of IBDG output fault current is proposed as

$$\theta_{IBDG}^{+/-} = 180° - \theta_{UG}^{+/-} - \delta_{PCC}^{+/-} \tag{6}$$

Considering the line impedance, the PCC voltage phase angle $\delta_{PCC}^{+/-}$ should meet the following requirement,

$$\delta_{PCC}^{+/-} > \delta_0^{+/-} \tag{7}$$

While,

$$\begin{aligned} \delta_{PCC}^{+/-} &> \delta_{ref}^{+/-} \\ \delta_0^{+/-} &< \delta_{ref}^{+/-} \end{aligned} \tag{8}$$

where $\delta_{PCC}^{+/-}$ and $\delta_0^{+/-}$ are the phase angel of PCC voltage and fault bus voltage, respectively. The $\delta_{ref}^{+/-}$ is the reference phase angle of V_{UG}. Generally speaking, $\delta_{ref}^{+/-}$ is set as 0 as a reference.

C. ICG STRATEGY

Under fault condition, the IBDGs need to have fault ride-through capability to keep in grid-connection state. According to the German E.ON NetZ code [22], the reactive output current for IBDG is estimated as

$$I_{IBDG(q)}^{+/-} = \begin{cases} 0, & U_0^+ \in (0.9U_N, 1.2U_N] \\ k_{FRT}^{+/-} \times (\dfrac{U_N - U_0^{+/-}}{U_N}) \times I_N, & \\ & U_0^+ \in (0.5U_N, 0.9U_N] \\ I_N, & U_0^+ \in (0, 0.5U_N] \end{cases} \tag{9}$$

where $k_{FRT}^{+/-}$ is the adjustment coefficient for FRT, $U_0^{+/-}$ is the fault voltage at fault bus, U_N is the normal voltage of utility grid, I_N is the normal current.

For the purpose to match the function of MCPAA and VPAD to achieve the negative contribution of IBDG fault current, its phase angle should be shifted to θ_{IBDG}. Thus, the active and reactive IBDG output current need to meet the following relationships,

$$\tan(\theta_{IBDG}^{+/-}) = \frac{I_{IBDG(q)}^{+/-}}{I_{IBDG(p)}^{+/-}} \tag{10}$$

where $I_{IBDG(p)}^{+/-}$ and $I_{IBDG(q)}^{+/-}$ are the positive and negative sequence of active and reactive IBDG output current.

Based on Clarke transformation theory, the PCC voltages in the stationary reference frame $(\alpha\beta)$ can be described as [31], [32]

$$u^+ = \begin{bmatrix} u_\alpha^+ \\ u_\beta^+ \end{bmatrix} = \begin{bmatrix} U^+ \cos(\omega t + \theta^+) \\ U^+ \sin(\omega t + \theta^+) \end{bmatrix}$$

$$u^- = \begin{bmatrix} u_\alpha^- \\ u_\beta^- \end{bmatrix} = \begin{bmatrix} U^- \cos(\omega t + \theta^-) \\ -U^- \sin(\omega t + \theta^-) \end{bmatrix} \tag{11}$$

where $U^+ = \sqrt{(u_\alpha^+)^2 + (u_\beta^+)^2}$, $U^- = \sqrt{(u_\alpha^-)^2 + (u_\beta^-)^2}$.

The injected active and reactive powers of IBDG is obtained as

$$\begin{bmatrix} P_{IBDG} \\ Q_{IBDG} \end{bmatrix} = \frac{3}{2} \begin{bmatrix} u_\alpha & u_\beta \\ u_\beta & -u_\alpha \end{bmatrix} \begin{bmatrix} i_{IBDG(\alpha)} \\ i_{IBDG(\beta)} \end{bmatrix} \tag{12}$$

According to (12), the IBDG inverter's output fault current can be described as [28], [33]

$$i_{IBDG(p\alpha)}^* = \frac{2}{3} \frac{u_\alpha^+ + u_\alpha^-}{(u_\alpha^+ + u_\alpha^-)^2 + (u_\beta^+ + u_\beta^-)^2} P_{IBDG}^*$$

$$i_{IBDG(p\beta)}^* = \frac{2}{3} \frac{u_\beta^+ + u_\beta^-}{(u_\alpha^+ + u_\alpha^-)^2 + (u_\beta^+ + u_\beta^-)^2} P_{IBDG}^*$$

$$i_{IBDG(q\alpha)}^* = \frac{2}{3} \frac{u_\beta^+ + u_\beta^-}{(u_\alpha^+ + u_\alpha^-)^2 + (u_\beta^+ + u_\beta^-)^2} Q_{IBDG}^*$$

$$i_{IBDG(q\beta)}^* = \frac{2}{3} \frac{-u_\alpha^+ - u_\alpha^-}{(u_\alpha^+ + u_\alpha^-)^2 + (u_\beta^+ + u_\beta^-)^2} Q_{IBDG}^* \tag{13}$$

where $i_{IBDG(p\alpha)}^*$, $i_{IBDG(p\beta)}^*$, $i_{IBDG(q\alpha)}^*$ and $i_{IBDG(q\beta)}^*$ are the reference of active and reactive current in the stationary reference frame $(\alpha\beta)$.

According to (9) and (10), the reference of injected active and reactive power in (13) is obtained as

$$P_{IBDG}^* = \frac{3}{2}(U^+ I_{IBDG(p)}^+ + U^- I_{IBDG(p)}^-)$$

$$Q_{IBDG}^* = \frac{3}{2}(U^+ I_{IBDG(q)}^+ + U^- I_{IBDG(q)}^-) \tag{14}$$

Under fault condition, the IBDG output current should also be limited below the safety threshold. In order to avoid suddenly tripping of inverter during FRT. The peak fault current of inverter output current is

$$\begin{aligned} I_{peak} &= \frac{2}{3}\sqrt{(I_{IBDG}^+)^2 + (I_{IBDG}^-)^2 + 2I_{IBDG}^+ I_{IBDG}^-} \\ &= \frac{2}{3}(I_{IBDG}^+ + I_{IBDG}^-) \\ &= \frac{2}{3}\sqrt{(I_{IBDG(p)}^+)^2 + (I_{IBDG(q)}^+)^2} \\ &\quad + \frac{2}{3}\sqrt{(I_{IBDG(p)}^-)^2 + (I_{IBDG(q)}^-)^2} \end{aligned} \tag{15}$$

where I_{peak} is the peak value of IBDG output current.

In order to avoid tripping of IBDG's inverter, the peak current should be limited by

$$\begin{bmatrix} i_{IBDG(a)}^* \\ i_{IBDG(b)}^* \\ i_{IBDG(c)}^* \end{bmatrix} = \frac{I_{max}}{I_{peak}}$$

$$\times \begin{bmatrix} i_{IBDG(p\alpha)}^* + i_{IBDG(q\alpha)}^* \\ -\dfrac{1}{2}(i_{IBDG(p\alpha)}^* + i_{IBDG(q\alpha)}^*) + \dfrac{\sqrt{3}}{2}(i_{IBDG(p\beta)}^* + i_{IBDG(q\beta)}^*) \\ -\dfrac{1}{2}(i_{IBDG(p\alpha)}^* + i_{IBDG(q\alpha)}^*) - \dfrac{\sqrt{3}}{2}(i_{IBDG(p\beta)}^* + i_{IBDG(q\beta)}^*) \end{bmatrix} \tag{16}$$

where I_{max} is the maximum current. the I_{max} is 2~3 times I_N in silicon devices [3], [4].

Considering the great tracking performance, the proportional-resonant (PR) controller is applied for tracking the positive and negative sequence of active and reactive output current in this article [34].
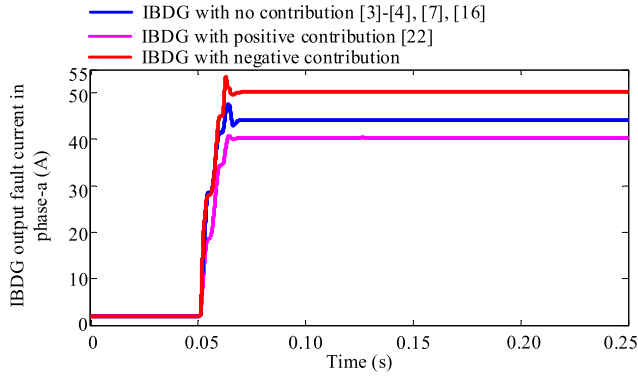
FIGURE 4. The FCNC method for IBDGs under grid fault.

FIGURE 5. The unbalanced fault voltage at fault bus.

The PR controller is described as

$$G(s) = k_{pI} + k_{rI} \frac{2\omega_c s}{s^2 + 2\omega_c s + \omega_0^2} \qquad (17)$$

where k_{pI} and k_{rI} are the proportional and resonant gain, ω_c is the cutoff frequency, while the ω_0 is the resonant frequency.

D. FCNC METHOD FOR IBDGs UNDER GRID FAULT

According to the analyses of Section III.A-C, the FCNC method for the negative contribution control of IBDGs under grid unbalanced fault is illustrated in Fig. 4. The FCNC method consists of MCPAA, VPAD and ICG strategies, which are embodied in different and related equations. The blue variable in Fig. 4 is the sampling and input signals of FCNC method.

IV. CASE STUDY

A. SYSTEM MODEL

The effectiveness of proposed FCNC method for IBDGs under grid unbalanced fault is tested and validated based on MATLAB/Simulink to achieve a negative contribution of IBDGs fault current on low-voltage ADN. To facilitate analysis, only one parallel IBDG is conducted, since the analyses of multiple IBDGs is similar to one. The unbalanced fault causes an unbalanced voltage sag, as displayed in Fig. 5. The fault occurs and the fault voltage drops at 0.05s. The contribution of proposed FCNC is to control the influence of IBDGs output fault current on system fault current. The network parameters are described in Table 1, and Table 2, respectively.

TABLE 1. The System Parameters.

Parameters	Symbol	Value	Unit
UG electrical distance	R_g / L_g	2.5 / 1.2	Ω / mH
IBDG electrical distance	R_l / L_l	1.5 / 0.8	Ω / mH
DC capacitor	C_{dc}	40	μF
Impedance of LCL filter	R / L	0.01 / 0.5	Ω / mH
Capacitor of LCL filter	C_{filter}	40	μF
UG nominal voltage	U_g	311	V
DC voltage	u_{dc}	800	V
Nominal frequency	f	50	Hz
Cutoff angular frequency	ω_c	70	rad/s
Switching frequency	f_s	10	kHz

TABLE 2. The Control Parameters.

Parameters	Symbol	Value
FCNC with positive contribution of IBDG [22]	k_{FRT}^+ / k_{FRT}^-	2.2 / 3
FCNC with no contribution of IBDG [3]-[4], [7]	k_{FRT}^+ / k_{FRT}^-	2.5 / -1.2
FCNC with negative contribution of IBDG	k_{FRT}^+ / k_{FRT}^-	3.1 / -2.5

FIGURE 6. Phase angel of IBDG output fault current under different scenarios.

B. FCNC METHOD FOR IBDG FAULT CURRENT CONTRIBUTION ANALYSES

Based on the MCPAA and VPAD strategies in proposed FCNC method, the phase angle of IBDG output fault current under different scenarios (positive, negative and no contribution of fault current on system) is shown in Fig. 6. In the scenario of positive contribution [22], the IBDG fault current angle does not needed to be shifted but only needed to satisfy the reactive and active current requirement for conventional FRT. The IBDG fault current's angle is small in this scenario, which can be also verified in the point A in Fig. 3(a). In the scenario of positive contribution [3], [4], [7], [16], the IBDG fault current's angle should be shift to point B in Fig. 3(a), and the phase angle is higher than its in scenario of positive contribution. In the scenario of negative contribution, the IBDG fault current's angle is shifted to the point C in Fig. 3(a). The IBDG fault current's phase angel is opposite to the utility grid fault current, and the addition for the phase angle of these two current components is 180°. In these three scenarios, the IBDG fault current's angle with negative contribution is largest, since the large phase angle is needed to be shifted to reduce the system fault current below than utility grid fault current.

FIGURE 7. Amplitude of IBDG output fault current in *phase-a* under different scenarios.

FIGURE 8. Amplitude of IBDG output fault current in *phase-c* under different scenarios.

FIGURE 9. Amplitude of system fault current in *phase-a* under different scenarios.

FIGURE 10. Amplitude of system fault current in *phase-c* under different scenarios.

TABLE 3. Comparison of Proposed and Existing Method.

Amplitude of fault current	Phase-a	Phase-b	Phase-c
Utility grid fault current (A)	296	128	128
IBDG fault current with positive contribution (A)	40	21	21
IBDG fault current with no contribution (A)	44	26	26
IBDG fault current with negative contribution (A)	51	33	33
System fault current with positive contribution (A)	340	150	150
System fault current with no contribution (A)	300	130	130
System fault current with negative contribution (A)	250	101	101

According to the unbalanced fault voltage in Fig. 5, and considering that the amplitude of *phase-b* and *phase-c* is the same, we focus on showing the *phase-a* and *phase-c* current to verify the effectiveness of FCNC method.

The amplitude of IBDG output fault currents in *phase-a* and *phase-c* under different scenarios are displayed in Fig. 7-8. The IBDG fault current amplitude in *phase-a* in the same scenario is larger than that in *phase-c*, since the fault voltage in *phase-a* is smaller than that in *phase-c*. In the scenario of positive contribution, the IBDG output fault current amplitude is smallest, since the active and reactive currents are only injected for conventional FRT requirement, without needing for additional phase angel adjustment. In the scenario of no contribution, the IBDG fault current amplitude should be higher to compensate the additional phase angle adjustment to make the system fault current equal the utility fault current. The greater the angle adjustment, the greater the amplitude of IBDG output fault current is needed for FRT to reduce the system fault current lower than utility grid fault current. Therefore, in the scenario of negative contribution, the IBDG output fault current amplitude will be largest.

The amplitude of system fault currents in *phase-a* and *phase-c* under different scenarios are shown in Fig. 9-10. The amplitude of system fault current in *phase-a* in the same scenario is larger than that in *phase-c*, since the fault voltage in *phase-a* is smaller than in *phase-c*. In the scenario of positive contribution, the system fault current amplitude is
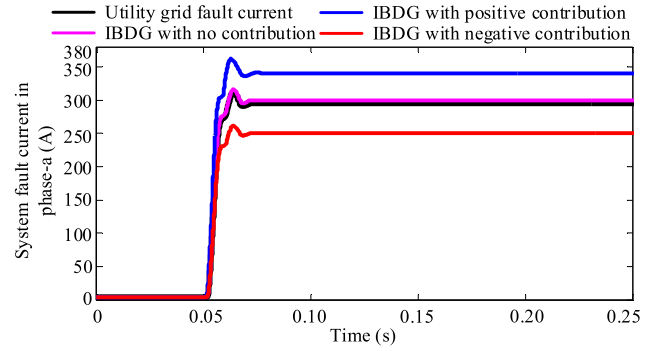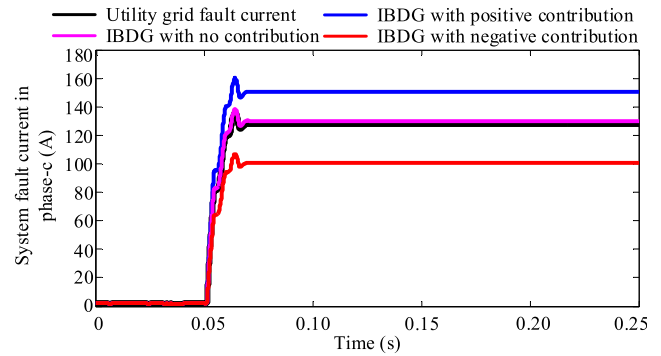
larger than that of utility grid fault current, since it is increased by the injected IBDG fault current. In the scenario of no contribution, the system fault current amplitude is almost the same as that of utility grid, since the injected IBDG fault current will not raise the system fault current amplitude. In the scenario of negative contribution, the system fault current amplitude is lower than that of utility grid, since the injected IBDG fault current will decrease the system fault current amplitude. The reason why the system fault current amplitude is respectively larger, equal and lower than that of utility grid under the positive, no, and negative contribution scenario, is that the adjustment of phase angle of IBDG output fault current has different impact on the system fault current, which is also displayed in Fig. 3.

Based on above analyses, the amplitude of fault currents under different scenario are shown in Table 3. The system fault current is the sum of utility grid fault current and IBDG fault current. It can be found that the IBDG fault current

increases sequentially under the scenario of positive, no and negative contribution, because of the adjustment size of phase angel. The system fault current in the scenario of positive, no and negative contribution decreases sequentially, due to the phase angel impact of IBDG fault current. According to the proposed FCNC method, the system fault current amplitude is smallest, and lower than the utility grid fault current.

V. CONCLUSION

Under the grid unbalanced fault condition, considering the increasing high-level system fault current due to large amount of the embedded IBDGs in ADN, the FCNC method is proposed to reduce the system fault current lower than the utility grid fault current. In contrary to the existing method that IBDGs provide varying degrees of positive or no contribution to system fault current, the proposed FCNC method can provide negative contribution of IBDG fault current to system. In the proposed method, the MCPAA strategy is conducted for IBDGs to maximize its negative contribution, thus to minimize the system fault current. The VPAD strategy is also formulated by considering the voltage angle difference on the electrical distance between IBDGs and fault bus. Extensive simulation test results have validated the effectiveness of proposed FCNC method to make the system fault current lower than the utility grid fault current. Considering that the FCNC method can reduce the fault current in ADN lower than that in traditional passive DN, the proposed FCNC will be much significant to the security and relay protection of grid.

REFERENCES

[1] Z. Li and M. Shahidehpour, "Privacy-preserving collaborative operation of networked microgrids with the local utility grid based on enhanced benders decomposition," *IEEE Trans. Smart Grid*, vol. 11, no. 3, pp. 2638–2651, May 2020.

[2] C. Li, X. Liu, W. Zhang, Y. Cao, X. Dong, F. Wang, and L. Li, "Assessment method and indexes of operating states classification for distribution system with distributed generations," *IEEE Trans. Smart Grid*, vol. 7, no. 1, pp. 481–490, Jan. 2016.

[3] N. Rajaei, M. H. Ahmed, M. M. A. Salama, and R. K. Varma, "Fault current management using inverter-based distributed generators in smart grids," *IEEE Trans. Smart Grid*, vol. 5, no. 5, pp. 2183–2193, Sep. 2014.

[4] N. Rajaei and M. M. A. Salama, "Management of fault current contribution of synchronous DGs using inverter-based DGs," *IEEE Trans. Smart Grid*, vol. 6, no. 6, pp. 3073–3081, Nov. 2015.

[5] W. Kou and D. Wei, "Fault ride through strategy of inverter-interfaced microgrids embedded in distributed network considering fault current management," *Sustain. Energy, Grids Netw.*, vol. 15, pp. 43–52, Sep. 2018.

[6] M. Ding, W. Wang, X. Wang, Y. Song, D. Chen, and M. Sun, "A review on the effect of large-scale PV generation on power systems," *Proc. CSEE*, vol. 34, no. 1, pp. 1–14, Jan. 2014.

[7] X. Liu, C. Li, M. Shahidehpour, Y. Gao, B. Zhou, Y. Zhang, J. Yi, and Y. Cao, "Fault current hierarchical limitation strategy for fault ride-through scheme of microgrid," *IEEE Trans. Smart Grid*, vol. 10, no. 6, pp. 6566–6579, Nov. 2019.

[8] W. Wan, Y. Li, B. Yan, M. Bragin, J. Philhower, P. Zhang, P. Luh, and G. Warner, "Active fault management for microgrids," in *Proc. IECON 44th Annu. Conf. IEEE Ind. Electron. Soc.*, Oct. 2018, pp. 1–6.

[9] M. Yousaf and T. Mahmood, "Protection coordination for a distribution system in the presence of distributed generation," *Turkish J. Electr. Eng. Comput. Sci.*, vol. 25, pp. 408–421, 2017.

[10] A. Beheshti, M. Shanbedi, and S. Z. Heris, "Heat transfer and rheological properties of transformer oil-oxidized MWCNT nanofluid," *J. Thermal Anal. Calorimetry*, vol. 118, no. 3, pp. 1451–1460, Dec. 2014.

[11] F. Coffele, A. Dysko, C. Booth, and G. Burt, "Quantitative analysis of network protection blinding for systems incorporating distributed generation," *IET Gener., Transmiss. Distrib.*, vol. 6, no. 12, pp. 1218–1224, Dec. 2012.

[12] C. J. Mozina, "Impact of smart grids and green power generation on distribution systems," *IEEE Trans. Ind. Appl.*, vol. 49, no. 3, pp. 1079–1090, May 2013.

[13] K. I. Jennett, A. J. Roscoe, C. D. Booth, and F. Coffele, "Investigation of the sympathetic tripping problem in power systems with large penetrations of distributed generation," *IET Gener., Transmiss. Distrib.*, vol. 9, no. 4, pp. 379–385, Mar. 2015.

[14] M. Han, W. Xie, W. Cao, W. Zhang, and J. Yang, "Application scenarios and system design of medium-voltage DC distribution network," *Autom. Electr. Power Syst.*, vol. 43, no. 23, pp. 1–11, Dec. 2019.

[15] Y. Jin, Y. Chen, Z. Lu, Q. Zhang, and R. Kang, "Cascading failure modeling for circuit systems using impedance networks: A current-flow redistribution approach," *IEEE Trans. Ind. Electron.*, vol. 68, no. 1, pp. 632–641, Jan. 2021.

[16] X. Liu, C. Li, M. Shahidehpour, X. Chen, J. Yi, Q. Wu, K. Sun, and B. Zhou, "Fault current mitigation and voltage support provision by microgrids with synchronous generators," *IEEE Trans. Smart Grid*, vol. 11, no. 4, pp. 2816–2831, Jul. 2020.

[17] *IEEE Standard for Interconnecting Distributed Resources With Electric Power Systems*, Standard 1547-2003, 2003.

[18] *IEEE Recommended Practice for Utility Interface of Photovoltaic (PV) Systems*, Standard 929-2000, 2000.

[19] *Static Inverter and Charge Controllers for Use in Photovoltaic Systems*, Standard UL 1741-1999, 2001.

[20] M. Tsili and S. Papathanassiou, "A review of grid code technical requirements for wind farms," *IET Renew. Power Generat.*, vol. 3, no. 3, pp. 308–332, Sep. 2009.

[21] V. Vekhande, K. V. K., and B. G. Fernandes, "Control of three-phase bidirectional current-source converter to inject balanced three-phase currents under unbalanced grid voltage condition," *IEEE Trans. Power Electron.*, vol. 31, no. 9, pp. 6719–6737, Sep. 2016.

[22] X. Zhao, J. M. Guerrero, M. Savaghebi, J. C. Vasquez, X. Wu, and K. Sun, "Low-voltage ride-through operation of power converters in grid-interactive microgrids by using negative-sequence droop control," *IEEE Trans. Power Electron.*, vol. 32, no. 4, pp. 3128–3142, Apr. 2017.

[23] J. Miret, A. Camacho, M. Castilla, L. G. de Vicuna, and J. Matas, "Control scheme with voltage support capability for distributed generation inverters under voltage sags," *IEEE Trans. Power Electron.*, vol. 28, no. 11, pp. 5252–5262, Nov. 2013.

[24] H. Nourmohamadi, M. Sabahi, E. Babaei, and M. Abapour, "A new structure of fault current limiter based on the system impedance with fast eliminating method and simple control procedure," *IEEE Trans. Ind. Electron.*, vol. 65, no. 1, pp. 261–269, Jan. 2018.

[25] P. Yu, B. Venkatesh, A. Yazdani, and B. N. Singh, "Optimal location and sizing of fault current limiters in mesh networks using iterative mixed integer nonlinear programming," *IEEE Trans. Power Syst.*, vol. 31, no. 6, pp. 4776–4783, Nov. 2016.

[26] M. Abdolkarimzadeh, M. Nazari-Heris, M. Abapour, and M. Sabahi, "A bridge-type fault current limiter for energy management of AC/DC microgrids," *IEEE Trans. Power Electron.*, vol. 32, no. 12, pp. 9043–9050, Dec. 2017.

[27] H. Nourmohamadi, M. Nazari-Heris, M. Sabahi, and M. Abapour, "A novel structure for bridge-type fault current limiter: Capacitor-based nonsuperconducting FCL," *IEEE Trans. Power Electron.*, vol. 33, no. 4, pp. 3044–3051, Apr. 2018.

[28] X. Guo, W. Liu, and Z. Lu, "Flexible power regulation and current-limited control of the grid-connected inverter under unbalanced grid voltage faults," *IEEE Trans. Ind. Electron.*, vol. 64, no. 9, pp. 7425–7432, Sep. 2017.

[29] F. Nejabatkhah, Y. W. Li, K. Sun, and R. Zhang, "Active power oscillation cancelation with peak current sharing in parallel interfacing converters under unbalanced voltage," *IEEE Trans. Power Electron.*, vol. 33, no. 12, pp. 10200–10214, Dec. 2018.

[30] A. Camacho, M. Castilla, J. Miret, A. Borrell, and L. G. de Vicuna, "Active and reactive power strategies with peak current limitation for distributed generation inverters during unbalanced grid faults," *IEEE Trans. Ind. Electron.*, vol. 62, no. 3, pp. 1515–1525, Mar. 2015.

[31] A. Camacho, M. Castilla, J. Miret, L. G. de Vicuna, and R. Guzman, "Positive and negative sequence control strategies to maximize the voltage support in Resistive–Inductive grids during grid faults," *IEEE Trans. Power Electron.*, vol. 33, no. 6, pp. 5362–5373, Jun. 2018.

[32] M. M. Shabestary and Y. A.-R.-I. Mohamed, "Analytical expressions for multiobjective optimization of converter-based DG operation under unbalanced grid conditions," *IEEE Trans. Power Electron.*, vol. 32, no. 9, pp. 7284–7296, Sep. 2017.

[33] X. Liu, X. Chen, C. Li, M. Shahidehpour, K. Sun, Y. Cao, C. Chen, and B. Zhou, "Multi-stage voltage support optimization for microgrids with multiple distributed generation units," *IEEE Trans. Smart Grid*, early access, Aug. 14, 2021, doi: 10.1109/TSG.2020.3016601.

[34] X. Chen, Y. Hou, and S. Y. R. Hui, "Distributed control of multiple electric springs for voltage control in microgrid," *IEEE Trans. Smart Grid*, vol. 8, no. 3, pp. 1350–1359, May 2017.

XUBIN LIU received the B.E. degree in automation from the College of Electrical Engineering, Northwest University for Nationalities, Lanzhou, China, in 2013, and the Ph.D. degree in electrical engineering from Hunan University, Changsha, China, in 2019.

He is currently a Postdoctoral Researcher with the School of Electrical and Electronic Engineering, Huazhong University of Science and Technology (HUST), Wuhan, China. His research interests include power system dispatch, self-healing of smart grid, and power electronics control.

• • •